https://dx.doi.org/10.21577/0103-5053.20220137

J. Braz. Chem. Soc., Vol. 34, No. 5, 673-683, 2023
©2023 Sociedade Brasileira de Química

Article

Synthesis, Characterization, and Anion Exchange Reactions of Zn_2Cr Layered Double Hydroxides Intercalated with Acetate and Chloride

Anne Raquel Sotiles,[a] Marco T. Grassi,[a] Mayara P. dos Santos,[a] Luis Gustavo S. Lameu[a] and Fernando Wypych[,a]*

[a]*Departamento de Química, Universidade Federal do Paraná, CP 19032, Jardim das Américas, 81531-980 Curitiba-PR, Brazil*

Layered double hydroxides (LDH) with the composition Zn_2Cr, intercalated with acetate and chloride ions were synthesized by co-precipitation with increasing pH and characterized by X-ray diffraction (XRD), Fourier-transform infrared spectroscopy (FTIR), scanning electron microscopy (SEM), energy dispersive spectroscopy (EDS) and inductively coupled plasma-optical emission spectrometry (ICP-OES). The samples synthesized at optimized pH showed XRD patterns with basal diffraction peaks typical of layered structures, with basal distances of 7.88 and 12.69 Å for intercalated chloride (Zn_2Cr/Cl) and acetate (Zn_2Cr/Ac), respectively. After optimization experiments, exchange reactions were performed with different anions, using an excess of five times the anions to be intercalated. Zn_2Cr/Cl was exchanged with CH_3COO^-, F^-, Br^-, I^-, SO_4^{2-} and NO_3^-, and Zn_2Cr/Ac was exchanged with F^-, Cl^-, Br^-, I^-, SO_4^{2-} and NO_3^-. Not all reactions were effective, indicating that among the evaluated anions, CH_3COO^- was preferred for exchange, mainly attributed to the pre-expansion with bigger anions, facilitating the exchange with smaller anions.

Keywords: layered double hydroxide, intercalation, chromium, exchange reactions

Introduction

Recently, the properties of two-dimensional materials have been gaining importance due to advances in nanoscience and nanotechnology in producing new combinations of materials with novel properties, expanding the range of applications.

Layered double hydroxides (LDH) are compounds belonging to this class of materials, especially those with brucite-like structures ($Mg(OH)_2$), in which Mg^{2+} cations are coordinated with six hydroxyls and the octahedra share edges to form two-dimensional layers, which are packed along the basal direction and held together with hydrogen bonds.[1] In the LDH structure, a partial replacement of divalent metals by trivalent metals occurs, generating an excess of positive charge in the layers, which are compensated by the intercalation of hydrated anions. The traditional family of LDHs is represented by the formula $[M^{2+}_{1-x}M^{3+}_x(OH)_2](A^{n-})_{x/n}{\cdot}yH_2O$, where M^{2+} and M^{3+} represent the metals present in the layer and $(A^{n-})_{x/n}{\cdot}yH_2O$ denotes the intercalated hydrated anions.[2,3] These compounds are attractive due to the wide range of applications, and although LDHs exist as minerals, it is possible to obtain them at a relatively low cost, using different synthetic approaches. Thus, it is important to study new phases aiming at new applications of these compounds.[4]

LDHs are known for their high anion exchange capacity (AEC) and the intercalation of different anions can provide different properties to the materials. Some anions have been widely studied, such as carbonate, nitrate, chloride and phosphate, and several anions have been cited as exchangeable, both organic and inorganic.[3,5]

Recently, some studies involving LDH intercalated with sulfate with the main formula $A(H_2O)_6[M^{2+}{}_6Al_3(OH)_{18}(SO_4)_2]{\cdot}6H_2O$ (M^{2+} = Mn, Mg, Zn, A^+ = Li, Na, K) have gained importance since they also present the intercalation of cations and have anion and/or cation exchange capacity.[6-9] However, there are still few reports in the literature of LDHs intercalated with some anions, as is the case of acetate, either the compound obtained by anion exchange or by direct synthesis.

In addition to the intercalated anions, the metals present in the layers also influence the properties of the material, and several combinations of divalent and trivalent metals

*e-mail: wypych@ufpr.br
Editor handled this article: Célia M. Ronconi (Associate)

have been reported[10,11] for applications as catalysts,[12,13] controlled release fertilizers,[14,15] as functional fillers in polymeric nanocomposites, emulsion stabilizers[16,17] and for environmental remediation through adsorption or degradation of contaminants.[18-22]

An element less present in LDH structures is chromium (Cr^{3+}), since most of the compounds described are synthesized with different metals and using Al^{3+}. To expand knowledge of this class of layered materials, we synthesized compounds containing Zn/Cr in the Zn^{2+}:Cr^{3+} molar ratio of 2:1 and intercalated them with chloride and acetate, and then evaluated the compounds as exchangers of different anions.

Experimental

LDHs with Zn^{2+}:Cr^{3+} with molar ratios of 2:1 were synthesized by co-precipitation with increasing pH. First, experiments were performed to determine the best pH for the formation of crystalline compounds. Using the Zn_2Cr/Cl phase as an example, $ZnCl_2$ 97% (Vetec, Rio de Janeiro, Brazil), $CrCl_3$ 98% (Êxodo Científica, Sumaré, Brazil), and NaCl 98.5% (Reatec, Colombo, Brazil) were dissolved in 100 mL of Milli-Q (Millipore-simplicity UV, Bedford, USA) decarbonated water. The solution was kept at room temperature and slowly titrated with a solution of NaOH 98% (Sigma-Aldrich, Saint Louis, USA) 1 mol L^{-1} in an automatic glass titration reactor (UP Control, Porto Alegre, Brazil) operating at room temperature, coupled to a peristaltic pump and with pH control, under N_2 flow. All the chemicals were of analytical grade and used without further purifications.

The dispersions were removed from the reactor at desired pH and hydrothermally treated at 90 °C for 120 h in oven (Tecnal TE-395, Piracicaba, Brazil) and later the solids were separated by centrifugation (centrifuge Sigma 3-16P, rotor 11133, An der Unteren Söse, Germany) at 4000 rpm, repeatedly washed and redispersed in a portion of decarbonated and distilled water and finally dried at room temperature. The same procedure was performed for the Zn_2Cr/Ac phase, using $Zn(C_2H_3O_2)_2$ 99.5% (Química Moderna, Barueri, Brazil), CH_3COONa 99% (Alphatec, São José dos Pinhais, Brazil), and $Cr_3(OH)_2(CH_3CO_2)_7$ 99.5% (Carlo Erba, São Paulo, Brazil). The chemicals and the corresponding amounts used in the synthesis of the samples are presented in Table 1.

After determination of the optimal pH for the synthesis of more crystalline phases, the samples intercalated with chloride (Zn_2Cr/Cl) and acetate (Zn_2Cr/Ac) were again synthesized, and for the anion exchange reactions, an aqueous dispersion of the solid was magnetically stirred with excess of salts (five times the concentration of the intercalated anion) for 7 days at room temperature and under N_2 flow. The exchange time was optimized and to avoid the loss of water, the Becker containing the dispersion was protected with a polymeric film with small holes to release the N_2 flow.

The phase synthesized with acetate was exchanged with NaF 99% (Carlo Erba, São Paulo, Brazil), NaCl 98.5% (Reatec, Colombo, Brazil), KBr 99% (Sigma-Aldrich, Saint Louis, USA), NaI 99% (Riedel-de Haen, Seelze, Germany), $Li_2SO_4{\cdot}H_2O$ 98.5% (Reatec, Colombo, Brazil), and $NaNO_3$ 99% (F. Maia, Belo Horizonte, Brazil), while phase intercalated with chloride was exchanged with CH_3COONa, NaF, KBr, NaI, Li_2SO_4 and $NaNO_3$. After the reactions, the solid dispersions were centrifuged at 4000 rpm, the solids washed several times with decarbonated and distilled water and dried at room temperature.

The materials were characterized by X-ray diffraction (XRD) using a Shimadzu XRD-6000 diffractometer (Kyoto, Japan) with Cu Kα 1.5418 Å radiation. The slurry obtained after the last centrifugation and washing procedure was dropped on the glass sample holder and allowed to dry at room temperature to form a film. The analyses were performed using voltage of 40 kV and current of 30 mA, with a dwell time of 2° min^{-1} and step of 0.02° in 2θ.

Fourier-transform infrared (FTIR) spectra were obtained in transmission mode using a Bruker Vertex 70 spectrophotometer (Billerica, USA) with KBr pellets containing around 1% (m/m) of the sample. The spectra were collected from 400-4000 cm^{-1}, with 32 scans and using a resolution of 2 cm^{-1}.

Scanning electron microscopy (SEM) image were obtained with a Tescan Vega3LMU microscope with AZ Tech software. The samples were deposited on copper tapes, and after collecting the energy-dispersive X-ray (EDS) spectra, the samples were sputtered with a thin gold layer to obtain the SEM images.

The elements were quantified with a Thermo Fisher Scientific inductively coupled plasma atomic emission (ICP-OES) spectrometer (model iCAP 6500) (Waltham,

Table 1. Chemicals, amounts and conditions used during the syntheses

Obtained phase	Divalent metal salt / mmol	Trivalent metal salt / mmol	Sodium salt / mmol	Initial pH	Final pH
Zn_2Cr/Cl	$ZnCl_2$ (31.250)	$CrCl_3$ (15.628)	NaCl (5.236)	3.35	6.47
Zn_2Cr/Ac	$Zn(C_2H_3O_2)_2$(29.088)	$Cr_3(OH)_2(CH_3CO_2)_7$(4.834)	$NaC_2H_3O_2$ (4.839)	6.03	8.95

USA) with the Thermo Scientific iTeVa software version 1.2.0.30. The samples were dissolved in a solution containing 1.0% v/v of HNO_3 65% (Alphatec, São José dos Pinhais, Brazil), in Milli-Q water and the data were collected in duplicate. The analytical lines used were 267.7 nm for chromium and 213.8 nm for zinc.

Results and Discussion

The XRD patterns of Zn_2Cr/Cl (Figure 1A) and Zn_2Cr/Ac (Figure 1B) showed series of basal peaks characteristic of layered structures.

The Zn_2Cr/Cl samples (Figure 1A) synthesized in the pH range of 6.05 to 9.63 presented the same pattern reported for samples intercalated with chloride and synthesized with different M^{2+} and M^{3+} metals with composition $M^{2+}_6M^{3+}_2(OH)_{16}Cl_2{\cdot}4H_2O$ (M^{2+} = Mg, Ni, Zn, Co, Mn; M^{3+} = Al, Fe), or in short, $[M^{2+}_{1-x}M^{3+}_x(OH)_2](A^{n-})_{x/n}{\cdot}yH_2O$.[23] Three basal diffraction peaks were observed, and the basal distance of 7.76 Å was the same for the different pH values, which is consistent with the intercalation of the chloride anion as previously reported.[24-26] The low crystallinity (or the small number of packed layers along the basal direction) did not vary greatly with the change of synthesis pH and small intensity diffraction peaks were observed in the region of 60° (in 2θ) but the polytype could not be identified. Due to this low crystallinity and stacking disorder, the cell parameters along the layers could not be determined.

Also, Cr^{3+} oligomeric species were present in the pH range of 6 to 8, affecting the formation of crystalline LDH and resulting in materials with layer-stacking faults.[27]

The Zn_2Cr/Ac samples (Figure 1B) synthesized in the pH range of 7.94 to 11.07 also presented three broad diffraction peaks with basal distances ranging from 11.77 to 12.28 Å, close to those reported in the literature for LDHs with different double and triple charged metal combinations and intercalated with acetate.[28-30] Based on the high intensity and the sharp basal diffractions peaks, the crystallinity varied a lot with changing pH, being most crystalline at pH close to 9 (Figure 1Bc).

At higher pH (Figure 1Bg), a small diffraction peak (indicated with an asterisk) was observed with a basal distance of around 21 Å, which can be attributed to the intercalation of Cr^{3+} complexes like $[Cr(OH)_4]^-$, the predominant species at pH = 11.[31]

The FTIR spectra (Figure 2) showed the same pattern for the different pH values of the same sample, Zn_2Cr/Cl (Figure 2A) or Zn_2Cr/Ac (Figure 2B).

For all samples, the characteristic bands of the LDH structure were identified, such as the vibrations of the M–O bonds in the region below 750 cm^{-1} and the bands in the region of 3400 cm^{-1} and at 1620 cm^{-1}, attributed to the stretching of the O–H bonds and bending of the water molecules, respectively.[32-34] The FTIR spectra of the Zn_2Cr/Cl samples (Figure 2A) also had bands in the region of 1360 cm^{-1}, indicating small contamination with carbonate, not observed through XRD since both basal distances were similar and the diffractions peaks overlapped.[35-37]

In addition to the characteristic bands of the LDH structure, in the spectra of the Zn_2Cr/Ac samples (Figure 2B) it was possible to identify bands at 1410 and 1560 cm^{-1}, attributed, respectively, to the symmetric and antisymmetric stretching of C–O bonds of carboxylate groups and bands attributed to C–C (930 cm^{-1}) and C–H bonds (2890, 2830, 1340, 1047 and 1020 cm^{-1}), confirming the presence of the intercalated acetate anions.[28,37-40]

According to the higher intensity and sharper diffraction peaks in the XRD patterns, indicating a bigger number of packed layers and consequently higher crystallinity, the best pH values for the syntheses were close to 6 for the Zn_2Cr/Cl and close to 9 for Zn_2Cr/Ac, using the chemical concentrations and the synthesis procedure of the present

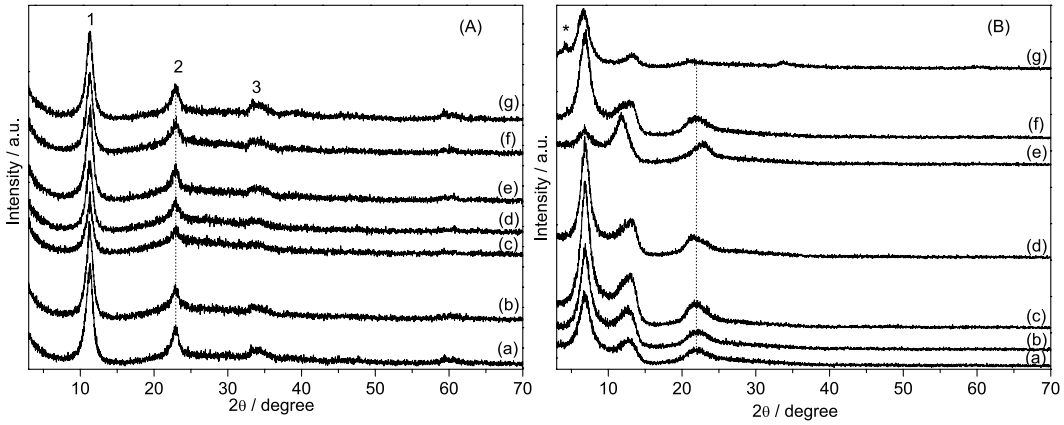

Figure 1. XRD patterns of Zn_2Cr/Cl synthesized at pH 6.05 (a), 6.90 (b), 7.85 (c), 8.29 (d), 8.66 (e), 9.06 (f) and 9.63 (g) (A) and Zn_2Cr/Ac (B) synthesized at pH 7.94 (a), 8.50 (b), 9.07 (c), 9.47 (d), 10.00 (e), 10.57 (f) and 11.07 (g). *Phase probably intercalated with $[Cr(OH)_4]^-$.

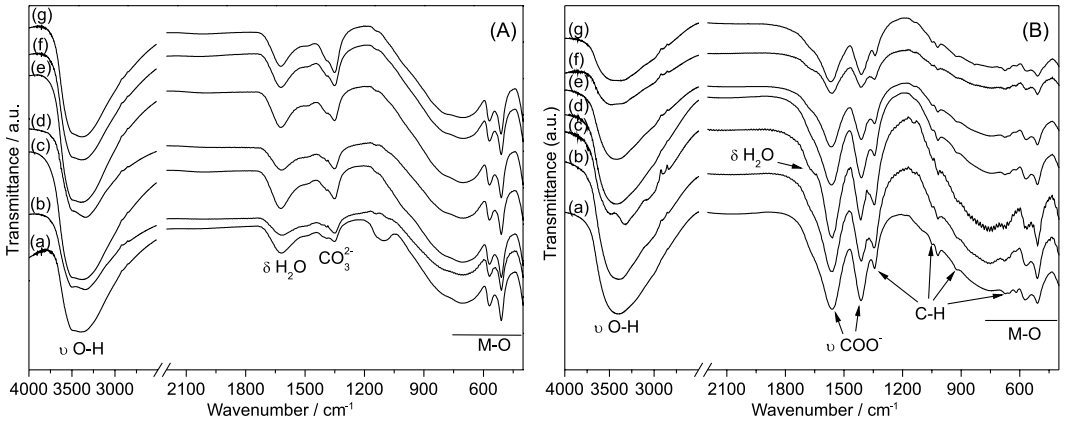

Figure 2. FTIR (KBr pellets) spectra of Zn_2Cr/Cl (A) synthesized at pH 6.05 (a), 6.90 (b), 7.85 (c), 8.29 (d), 8.66 (e), 9.06 (f) and 9.63 (g) and Zn_2Cr/Ac (B) synthesized at pH 7.94 (a), 8.50 (b), 9.07 (c), 9.47 (d), 10.00 (e), 10.57 (f) and 11.07 (g).

work. The samples were again synthesized at the optimized pH values, and from these, anion exchange reactions were performed using different anions. The XRD patterns and FTIR spectra of the phases synthesized at the optimized pH values are shown in Figure 3.

With the optimized synthesis conditions, Zn_2Cr samples showed XRD patterns characteristic of layered compounds, with the presence of series of typical basal peaks. The Zn_2Cr/Cl phase (Figure 3Aa) presented a basal distance of 7.88 Å, which is consistent with the intercalation of chloride ions.[24,41] The Zn_2Cr/Ac phase synthesized at pH 8.95 (Figure 3Ab) had a basal distance of 12.69 Å, indicating the presence of acetate ions in a bilayer arrangement.[30,42]

The FTIR spectra (Figure 3B) presented a broad band in the region of 3400 cm^{-1}, attributed to the OH bond of the hydroxyls of the LDH structure and of the intercalated/adsorbed water molecules, in addition to a band at 1620 cm^{-1}, corresponding to the bending of the water molecules. The Zn_2Cr/Ac (Figure 3Bb) sample had bands at 568 and 618 cm^{-1}, attributed to the M–OH bonds, while the Zn_2Cr/Cl (Figure 3Ba) sample only had a band at 568 cm^{-1} and a broad band close to 600 cm^{-1}, possibly due to structural disorder, which was also detected by the noisier XRD pattern (Figure 3Aa). The other bands in the region below 750 cm^{-1} are related to the vibrations of the M–O bonds.[32,43] In addition to these bands, the Zn_2Cr/Ac phase (Figure 3Bb) presented bonds corresponding to the antisymmetric and symmetric stretching of the C–O bonds, attributed to the carboxylate groups, at 1570 and 1415 cm^{-1}, respectively, and the bands related to the vibrations of the C–H bond at 1340, 1051, 927 and 675 cm^{-1}.[38,44-46]

Despite the N_2 flow during synthesis and use of decarbonated water in the samples obtained at different pH values (Figure 2A), after synthesis at pH 6, the Zn_2Cr/Cl (Figure 3Ba) sample also had a small band in the region of 1365 cm^{-1}, attributed to carbonate contamination.

Figure 4 shows the X-ray diffraction patterns of Zn_2Cr/Cl before and after the anion exchange reactions. Zn_2Cr/Cl (Figure 4Aa) had a basal distance of 7.88 Å, and after the exchange with acetate (Figure 4Ab) the value remained practically constant (7.89 Å), indicating that the exchange reaction was not effective. However, after the anion

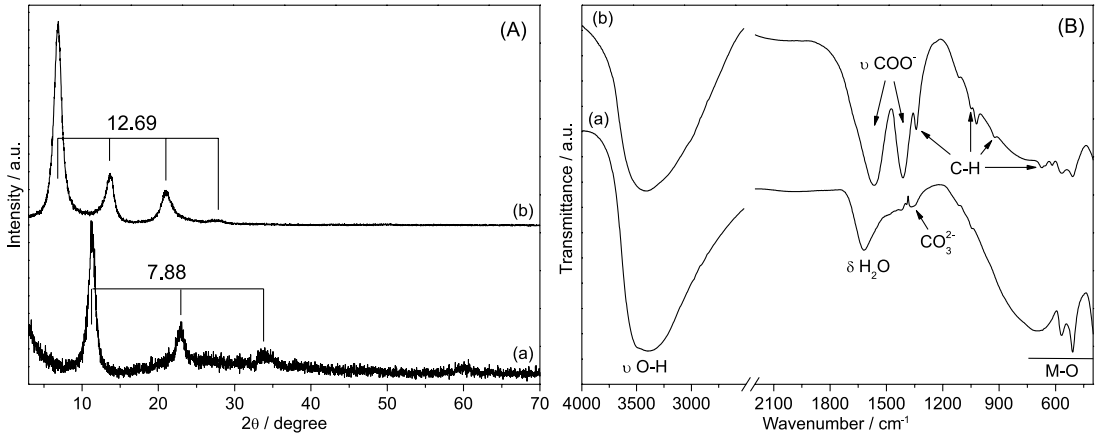

Figure 3. XRD patterns (A) and FTIR (KBr pellets) spectra (B) of Zn_2Cr/Cl synthesized at pH = 6.47 (a) and Zn_2Cr/Ac synthesized at pH = 8.95 (b). Values indicated in the XRD patterns are attributed to basal distances and indicated in Å.

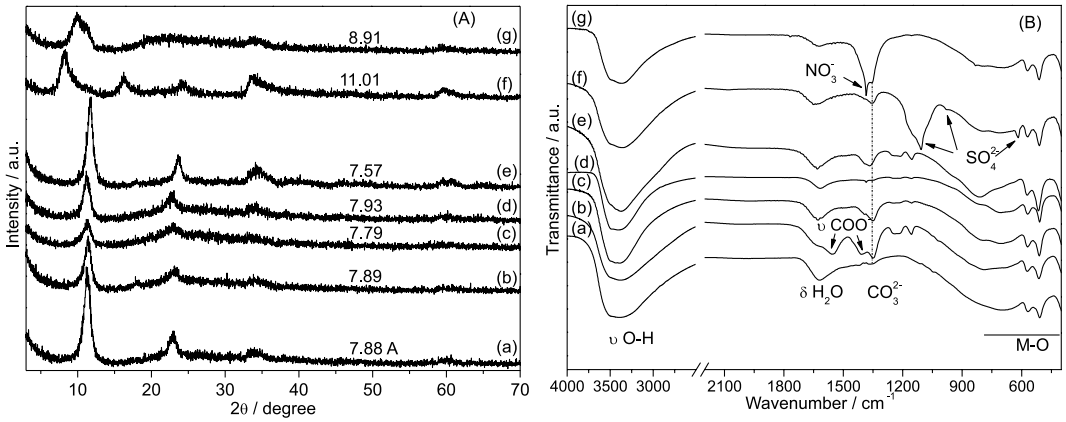

Figure 4. XRD patterns (A) and FTIR (KBr pellets) spectra (B) of Zn_2Cr/Cl before (a) and after exchange reactions with CH_3COONa (b), NaI (c), KBr (d), NaF (e), Li_2SO_4 (f) and $NaNO_3$ (g). Values indicated in the XRD patterns are attributed to basal distances and indicated in Å.

exchange, the FTIR spectrum (Figures 4Ba and 4Bb) had bands at 1555 and 1410 cm^{-1},[39,40] indicating the presence of acetate, but probably only exchanged at the surface of the particles, not intercalated.

After the exchange reaction of chloride with iodide (Figure 4Ac), the obtained basal distance of 7.79 Å indicated the absence of reaction, since intercalated iodides have basal distance close to 8 Å, due the ionic radius of hydrated I^- (2.10 Å) (predicted basal distance = 4.8 + 2.10 × 2 = 9.02 Å) was greater than that of Cl^- (1.56Å) (predicted basal distance = 4.8 + 1.56 × 2 = 7.92 Å).[47]

The small change in the basal distance in relation to the precursor was associated with the exchange of chloride anions with some carbonate anions, and the broadening of the diffraction peaks hampered determination of the values. The contamination was confirmed by the FTIR spectra (Figure 4Bc), with the presence of a band at 1360 cm^{-1}, attributed to carbonate.[48] Carbonate contamination was observed in most of the cases, the exception being the bromide exchange sample.

In the case of the sample after the bromide exchange reaction (Figure 4Ad), the basal distance changed from 7.88 to 7.93 Å. This increase was attributed to the fact that the ionic radius of Br^- (1.80 Å) is greater than that of the Cl^- that was previously intercalated in the LDH structure.[49,50] The predicted basal distance of Br^- intercalated LDH would be 4.8 + 1.80 × 2 = 7.96 Å.[47] The same behavior has already been observed in other studies, where intercalation of bromide in LDH led to a greater basal distance than with Cl^- (around 8.1 Å).[51-53] The FTIR spectra showed no changes compared to the precursor Zn_2Cr/Cl (Figures 4Ba and 4Bd), as expected.

For the Zn_2Al/Cl after the exchange with F^-, there was a reduction in the basal distance in relation to the precursor phase (Figures 4Aa and 4Ae), since the ionic radius of the fluoride (1.11 Å) is smaller than that of chloride. The predicted basal distance of F^- intercalated LDH was 4.8 + 1.11 × 2 = 7.02 Å.[47] The basal distance of 7.57 Å after the exchange reaction was consistent with the literature.[54-56]

After the reaction with Li_2SO_4 (Figures 4A and 4Bf), the crystallinity decreased and the basal distance increased to 11.01 Å, indicating the presence of sulfate ions in the interlayer spaces, in the form of a double layer. It is difficult to predict the basal distance in this case since sulfate can be intercalated with variable numbers of water molecules, with the basal distance ranging from 7.1 to 11 Å.[47,57,58] The FTIR spectra also confirmed the anion replacement due to the presence of typical ν_1, ν_3 and ν_4 bands of the S–O bond at 1115, 980 and 617 cm^{-1}, respectively, characteristic of distorted octahedral symmetry.[51,57,59]

As reported for other Zn_2Cr-SO_4 layered double hydroxides,[27] SO_4^{2-} was probably intercalated with the C_3v symmetry where one of the S–O bonds was oriented parallel to the c-crystallographic axis. Probably these ions were disordered between the layers and the layers were tilted, reducing the crystallinity of the synthesized materials.

After the reaction with $NaNO_3$ (Figure 4Ag), an increase of the basal distance to 8.91 Å was also observed, which is consistent with the NO_3^- intercalation (predicted basal distance = 4.8 + 1.89 × 2 = 8.58 Å). This exchange was also confirmed by the FTIR spectra (Figure 4Bg), in which a band at 1382 cm^{-1} was present, attributed to the N–O bond.[33]

For the Zn_2Cr/Ac compound (basal distance of 12.69 Å), all samples showed decreased crystallinity after the anion exchange reactions (Figure 5A). There was a shift in the position of the basal diffraction peaks to 7.82 Å (Figures 5Aa and 5Ab), consistent with chloride intercalation.[60] After the abrupt reduction of the basal distance, the layers stacking faults and reduction of the sizes of the crystalline domains are expected, which broadens the basal diffraction peaks. Unlike the phase synthesized with Zn_2Cr/Cl, in the Zn_2Cr/Ac

phase (Figure 5Ac) the sample had a basal distance of 8.13 Å, indicating exchanged reactions with iodide. This value is close to the values reported for LDHs intercalated with iodide, which were also obtained by anion exchange reactions.[30,61,62]

For samples after exchange of acetate with bromide (Zn_2Cr/Ac-Br) and fluoride (Zn_2Cr/Ac-F), (Figures 5Ad and 5Ae), the obtained basal values of 7.95 Å and 7.59 Å also confirmed the exchange reactions.[50,52,63,64] In the case of the Zn_2Cr/Ac-Cl, Zn_2Cr/Ac-I, Zn_2Cr/Ac-Br and Zn_2Cr/Ac-F samples (Figures 5Bb, 5Bc, 5Bd, 5Be), the typical bands of acetate in the FTIR spectra were not observed, suggesting complete anionic exchange reactions.

The XRD patterns and the FTIR spectra of the sample after the exchange reaction with Li_2SO_4 (Figures 5Af and 5Bf) showed changes in relation to the precursor Zn_2Cr/Ac. In addition to the reduction in crystallinity, the basal distance changed to 9.70 Å. This result differed from the other values obtained for the sulfate intercalation in the different phases synthesized in this work and from the values of 11 and 8.9 Å reported in the literature for the basal distance of sulfate intercalated in Zn_2Cr LDH.[57,65]

The FTIR spectra (Figure 5Bf) of this sample confirmed the anion exchange due to the presence of typical bands attributed to sulfate, located at 1100, 980 and 620 cm^{-1}.[66-68] The same behavior was observed in the sample after exchanging chloride with nitrate. In the XRD pattern (Figure 5Ag), the diffraction peaks shifted to 8.78 Å. In addition, there was splitting of the first basal diffraction peak, with a new peak at 7.75 Å, indicating carbonate intercalation. The FTIR spectra (Figure 5Bg) showed a band located at 1380 cm^{-1}, attributed to nitrate, and this band had a shoulder on the right side, which is associated with overlapping of the carbonate band, corroborating the results of X-ray diffraction.[69,70]

The SEM images (Figure 6) indicated agglomerated platelet-like particles, typical of LDHs prepared by evaporating the slurry in the sample holder. The sample Zn_2Cr/Ac (Figure 6a) contained particles in the range of 1 μm and smaller, but the particles along the platelets were larger than those of Zn_2Cr/Cl (Figure 6h), which presented nanometric dimensions.

The particle sizes along the basal axis (or platelet-like particles thicknesses) were calculated through the Scherrer equation (Table 2) and the values ranged from 77 to 92 Å for the Zn_2Cr/Cl system in the whole pH range and from 42 to 72 Å for the Zn_2Cr/Ac system, again for the whole pH range. It is important to mention that raw data were used, without including the instrumental corrections, so the data are only estimated values. The number of packed layers could the calculated by dividing the thicknesses of the platelet-like particles by the basal distance, which is an indication of the distance between two adjacent layers (also the thickness of one layer plus the interlayer space) (Figure S1, Supplementary Information (SI) section). The number of packed layers was almost the same in the Zn_2Cr/Cl system in the whole pH range investigated, from 10 to 12 layers, while these values were in the range of 4 to 6 for the Zn_2Cr/Ac system.

As observed through the SEM images, during the exchange reactions performed with the Zn_2Cr/Ac sample, the particles had increased sizes along the platelets due to Ostwald ripening, since the reactions were processed in solution for 7 days at room temperature. The same effect was also observed in the sample Zn_2Cr/Cl (Figure 6h), except for the sample after exchange with KBr (Figure 6k), in which the particles were smaller and more compacted. Except for the sample exchanged with Li_2SO_4, the number of packed layers remained almost constant for the Zn_2Cr/Cl phases after the exchange reactions, while

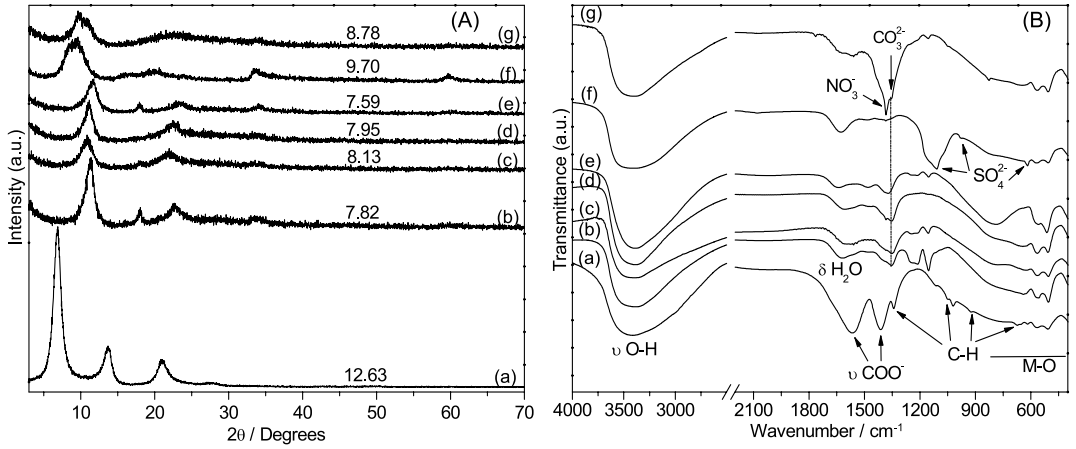

Figure 5. XRD patterns (A) and FTIR spectra (B) of Zn_2Cr/Ac before (a) and after exchange with NaCl (b), NaI (c), KBr (d), NaF (e), Li_2SO_4 (f) and $NaNO_3$ (g). Values indicated in the XRD patterns are attributed to basal distances and indicated in Å.

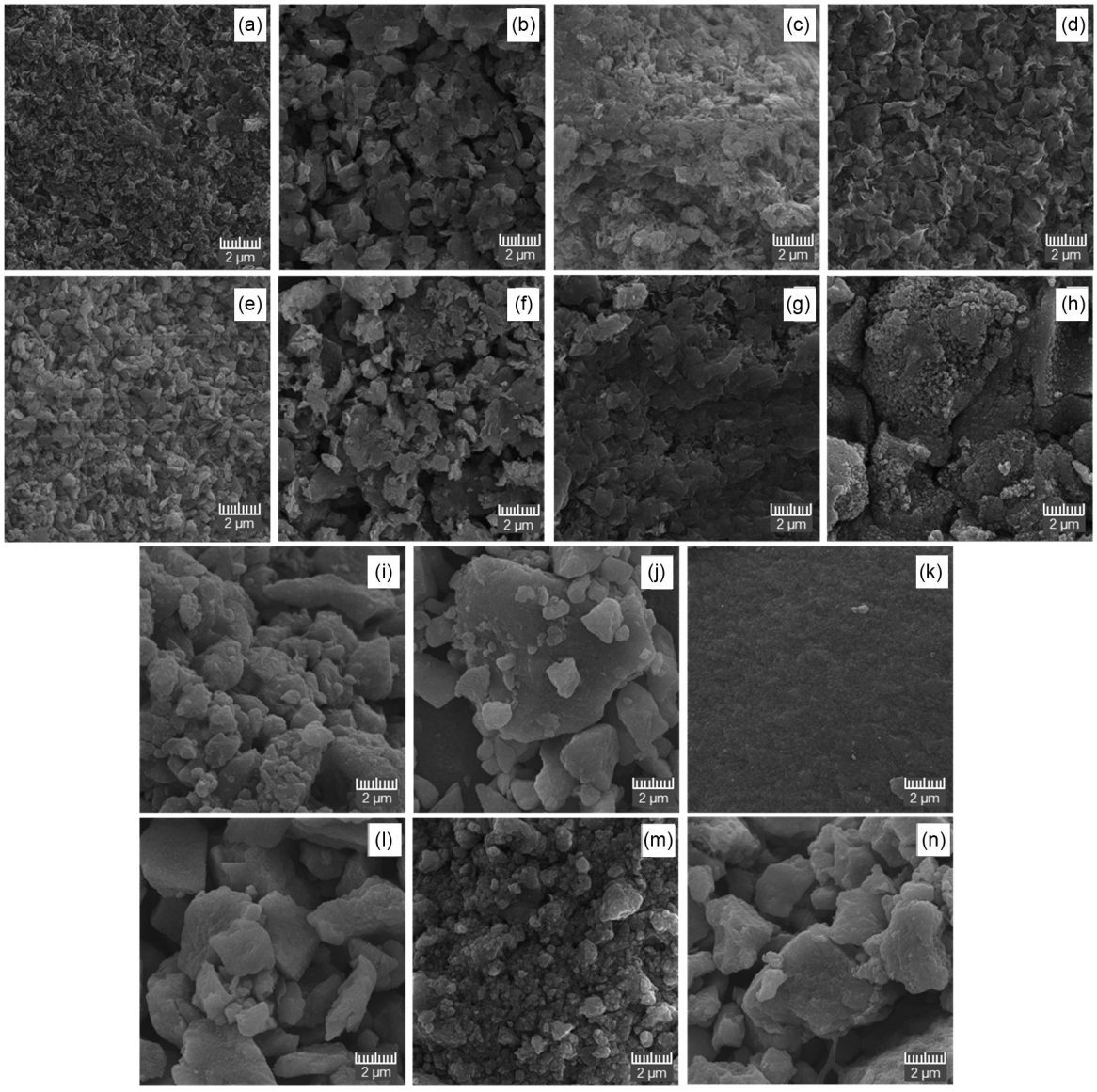

Figure 6. SEM images of Zn_2Cr/Ac before (a) and after the exchange reactions with NaCl (b), NaI (c), KBr (d), NaF (e), Li_2SO_4 (f), $NaNO_3$ (g) and, Zn_2Cr/Cl before (h) and after exchange with CH_3COONa (i), NaI (j), KBr (k), NaF (l), Li_2SO_4 (m) and $NaNO_3$ (n).

the number slightly increased in the Zn_2Cr/Ac system (Table 2).

The results obtained in the analysis of ICP-OES (Table 3) showed that in general the samples presented the expected compositions related to the M^{2+}:M^{3+} ideal molar ratios (Zn^{2+} = 0.667 and Cr^{3+} = 0.333).

The presence of sulfate ions was identified in the samples Zn_2Cr/Cl-SO_4 and Zn_2Cr/Ac-SO_4, confirming the exchange reactions. In addition, the presence of a small amount of Li was observed in these samples, but not the necessary amount of cations for a shigaite-like structure $[Na_{0.111}(H_2O)_{0.667}][Mn_{0.667}Al_{0.333}(OH)_2(SO_4)_{0.222}]$,[71] as described for $Na_{0.11}[Zn_{0.67}Cr_{0.33}(OH)_2(SO_4)_{0.22}]$.[72]

In spite of the smaller expected value for lithium, the amount of sulfate was also smaller than predicted for the shigaite-like structure but higher than predicted for the $[Zn_{0.667}Al_{0.333}(OH)_2](SO_4)_{0.167}.yH_2O$ structure, which led us to conclude that some extra sulfate anions were grafted to the layers' surface partially OH^- anions or even attached to layers through $-OH_2^{+\cdots}LiSO_4^-$ bonds, as previously reported.[8,73-76]

Since most intercalated anions could not be evaluated through ICP-OES analysis, qualitative EDS spectra were obtained for the samples (SI section), confirming the exchange reactions by the presence of typical signals of the respective intercalated anions.

No elements were observed in the region of 1 to 5 eV in Zn_2Cr/Ac (Figure S2, SI section), and after the exchange reactions, signals were present at 2.6 eV, attributed to chloride (Figure S3, SI section), at 4 eV, attributed to iodine

Table 2. Estimation of the particle sizes along the basal axis through the Scherrer equation and number of packed layers along the basal axis

Compound	Particle thickness[a] / Å	Number of packed layers	Compound	Particle thickness[a] / Å	Number of packed layers
Zn_2Cr/Cl-6.05	87	11	Zn_2Cr-Ac-7.94	53	4
Zn_2Cr/Cl-6.90	87	11	Zn_2Cr-Ac-8.50	60	5
Zn_2Cr/Cl-7.85	90	12	Zn_2Cr-Ac-9.07	60	5
Zn_2Cr/Cl-8.29	79	10	Zn_2Cr-Ac-9.47	67	5
Zn_2Cr/Cl-8.66	79	10	Zn_2Cr-Ac-10	–	–
Zn_2Cr/Cl-9.06	83	11	Zn_2Cr-Ac-10.57	42	3
Zn_2Cr/Cl-9.63	77	10	Zn_2Cr-Ac-11.07	59	4
Zn_2Cr/Cl-6.47	92	12	Zn_2Cr-Ac-8.95	72	6
Zn_2Cr/Cl-Ac	83	11	Zn_2Cr/Ac-Cl	70	9
Zn_2Cr/Cl-I	77	9	Zn_2Cr/Ac-I	56	7
Zn_2Cr/Cl-Br	86	11	Zn_2Cr/Ac-Br	71	9
Zn_2Cr/Cl-F	94	12	Zn_2Cr/Ac-F	58	8
Zn_2Cr/Cl-S	65	7	Zn_2Cr/Ac-S	–	–
Zn_2Cr/Cl-N	–	–	Zn_2Cr/Ac-N	–	–

[a]Along the basal axis; Zn_2Cr/Cl-S = Zn_2Cr/Cl-SO_4; Zn_2Cr/Cl-N = Zn_2Cr/Cl-NO_3; Zn_2Cr/Ac-S = Zn_2Cr/Ac-SO_4; Zn_2Cr/Ac-N = Zn_2Cr/Ac-NO_3.

Table 3. Compositions of the samples obtained by ICP-OES

Compound	Zn^{2+}	Cr^{3+}	A^{n-}, Li^+
Zn_2Cr/Cl	0.662	0.338	n.e.
Zn_2Cr/Cl-Ac	0.648	0.352	n.e.
Zn_2Cr/Cl-NaI	0.658	0.342	n.e.
Zn_2Cr/Cl-KBr	0.668	0.332	n.e.
Zn_2Cr/Cl-NaF	0.654	0.356	n.e.
Zn_2Cr/Cl-Li_2SO_4	0.642	0.358	0.187 (0.222;[a] 0.167);[b] Li = 0.009 (0.111)[a]
Zn_2Cr/Cl-$NaNO_3$	0.659	0.341	n.e.
Zn_2Cr/Ac	0.652	0.348	n.e.
Zn_2Cr/Ac-NaCl	0.662	0.338	n.e.
Zn_2Cr/Ac-NaI	0.668	0.332	n.e.
Zn_2Cr/Ac-KBr	0.669	0.331	n.e.
Zn_2Cr/Ac-NaF	0.661	0.339	n.e.
Zn_2Cr/Ac-Li_2SO_4	0.675	0.325	0.191 (0.222;[a] 0.167);[b] Li = 0.015 (0.111)[a]
Zn_2Cr/Ac-$NaNO_3$	0.685	0.315	n.e.

A^{n-} = anion; n.e.: not evaluated; expected values for LDH with the composition [a]$Na_{0.111}[Zn_{0.667}Cr_{0.333}(OH)_2(SO_4)_{0.222}]$or [b]$[Zn_{0.667}Al_{0.333}(OH)_2]\ (SO_4)_{0.167}.yH_2O$.

(Figure S4, SI section), at 1.5 eV, attributed to bromide (Figure S5, SI section), at 0.7 eV, attributed to fluoride (Figure S6, SI section), at 2.3 eV, attributed to sulfur from sulfate (Figure S7, SI section), and at 0.4 eV when exchanged with $NaNO_3$ (Figure S8, SI section).

For the synthesized Zn_2Cr/Cl sample, a signal attributed to chloride was observed at 2.6 eV (Figure S9, SI section). This signal was still present in most samples after the exchange reactions and had greater intensity in samples in which anion substitutions were not observed by XRD analysis, as was the case of Zn_2Cr/Cl-Ac (Figure S10, SI section) and Zn_2Cr/Cl-NaI (Figure S11, SI section). Although in the EDS spectrum of the latter, the signals referring to iodide appeared in the region of 3.5-4.5 eV, indicating there was a partial exchange, but not enough to change the basal parameter to values consistent with the intercalation of iodide ions, therefore being considered negligible. For the other samples after the exchange reactions, signals were observed at 1.5 eV, attributed to bromide (Figure S12, SI section), at 0.7 eV, attributed to fluoride (Figure S13, SI section), at 2.3 eV, attributed to sulfur after exchange with Li_2SO_4 (Figure S14, SI section), and at 0.4 eV, attributed to nitrogen after exchange with $NaNO_3$ (Figure S15, SI section).

For the sample Zn_2Cr/Cl, the anion exchange reactions occurred when the sample was added to solutions containing bromide, fluoride, sulfate, and nitrate anions. Furthermore, there was partial substitution by acetate ions and absence of reactions when iodine was used. For the sample synthesized with acetate, Zn_2Cr/Ac, anion exchange reactions occurred in all cases when the sample was added to solutions containing fluoride, chloride, iodide, bromide, sulfate, and nitrate anions.

The series of anionic stabilization in the interlayer space in the order $CO_3^{2-} > SO_4^{2-} > OH^- > F^- > Cl^- > Br^- > NO_3^- > I^-$,[24] indicated LDH intercalated with Cl^- were likely replaced with Br^-, SO_4^{2-} and NO_3^-. However, the occurrence of unfavorable exchange reactions can be explained by the presence of an excess of the anions

of interest (five times in relation to the intercalated anions). In addition, sulfate and chloride are very close in the series, facilitating anion exchange, which has been observed in other studies.[77,78] Regarding acetate, which in all cases was exchanged for other anions, our results indicated it was the least stable among the evaluated anions, so its position in the series was $CO_3^{2-} > SO_4^{2-} > OH^- > F^- > Cl^- > Br^- > NO_3^- > I^- > CH_3COO^-$.

Conclusions

Layered double hydroxides of Zn_2Cr intercalated with chloride (Zn_2Cr-Cl) and acetate (Zn_2Cr-Ac) were successfully synthesized by co-precipitation with increasing pH, followed by hydrothermal ripening at 90 °C. To obtain phases with the best crystallinity of the precipitated materials, optimization of the synthesis was carried out at different pH values, and after determining the best value of pH, new syntheses were performed for the two compositions.

XRD patterns indicated that Zn_2Cr/Cl and Zn_2Cr/Ac had respective basal distances of 7.88 and 12.69 Å, consistent with the intercalation of chloride and acetate ions. The FTIR spectra showed the characteristic bands of the structure of the compounds, in addition to the bands attributed to the acetate ions, and a small contamination with carbonate in Zn_2Cr/Cl. The results obtained by XRD, FTIR and EDS showed the effectiveness of the exchange reactions. In general, there was a reduction in the crystallinity of the compounds, but the particles were bigger along the platelet particles. The basal distances increased or decreased as a function of the size of the ionic radius of the intercalated anions.

The results of ICP-OES indicated a molar ratio close to 2:1, according to the amounts used in the syntheses. Also, sulfate and lithium contents obtained by ICP-OES analyses after anion exchange were lower than expected for a shigaite-like composition $[Na_{0.111}(H_2O)_{0.667}][Mn_{0.667}Al_{0.333}(OH)_2(SO_4)_{0.222}]$.[77] However, the sulfate contents were above the values for a traditional LDH structure $[Zn_{0.667}Al_{0.333}(OH)_2](SO_4)_{0.167}.yH_2O$, indicating that the last composition is possible when part of the hydroxide anions are replaced with sulfate, or the excess of sulfate is retained through $-OH_2^{+\cdots}SO_4^{2-}$ bonds.

The phases Zn_2Cr/Cl and Zn_2Cr/Ac could not be converted to shigaite-like compounds with the composition $[Na_{0.111}(H_2O)_{0.667}][Mn_{0.667}Al_{0.333}(OH)_2(SO_4)_{0.222}]$, as reported for Mn_2Al layered double hydroxide,[77] but the question is still open if similar compounds can be directly obtained by co-precipitation of Cr, Al and alkali metal salts in the presence of sulfate, carbonate, vanadate, molybdate or other divalent anions.

For both the Zn_2Cr/Cl and Zn_2Cr/Ac samples, exchanges were achieved with bromide, fluoride, sulfate, and nitrate. In addition to these, in Zn_2Cr/Cl there was partial exchange with acetate, and for Zn_2Cr/Ac there were also exchanges with chloride and iodide, indicating that the acetate anion is the most labile among the evaluated anions.

The synthesized compounds are under investigation as semiconductors for photocatalytic degradation of substrates of environmental interest, results that will be the subject of future publications.

Supplementary Information

Supplementary information is available free of charge at http://jbcs.sbq.org.br as PDF file.

Acknowledgments

This study was financed in part by the Office to Coordinate Improvement of University Personnel (CAPES - Finance Code 001), the National Council for Scientific and Technological Development (CNPq, grant 300988/2019-2); Financier of Studies and Projects (FINEP). ARS thanks CNPq for the postdoctoral scholarship (process 163817/2020-0) and Centro de Microscopia Eletrônica - CME/UFPR for the SEM/EDS analyses.

References

1. Arizaga, G. G. C.; Mangrich, A. S.; Gardolinski, J. E. F. C.; Wypych, F.; *J. Colloid Interface Sci.* **2008**, *320*, 168. [Crossref]
2. Crepaldi, E. L.; Pavan, P. C.; Valim, J. B.; *J. Braz. Chem. Soc.* **2000**, *11*, 64. [Crossref]
3. Bukhtiyarova, M. V.; *J. Solid State Chem.* **2019**, *269*, 494. [Crossref]
4. Caporale, A. G.; Pigna, M.; Azam, S. M. G. G.; Sommella, A.; Rao, M. A.; Violante, A.; *Chem. Eng. J.* **2013**, *225*, 704. [Crossref]
5. Benício, L. P. F.; Eulálio, D.; Guimarães, L. M.; Pinto, F. G.; da Costa, L. M.; Tronto, J.; *Mater. Res.* **2018**, *21*, e20171004. [Crossref]
6. Sotiles, A. R.; Baika, L. M.; Grassi, M. T.; Wypych, F.; *J. Am. Chem. Soc.* **2019**, *141*, 531. [Crossref]
7. Sotiles, A. R.; Gomez, N. A. G.; dos Santos, M. P.; Grassi, M. T.; Wypych, F.; *Appl. Clay Sci.* **2019**, *181*, 105217. [Crossref]
8. Gomez, N. A. G.; Sotiles, A. R.; Wypych, F.; *Appl. Clay Sci.* **2020**, *193*, 105658. [Crossref]
9. Sotiles, A. R.; Wypych, F.; *J. Braz. Chem. Soc.* **2022**, *33*, 74. [Crossref]
10. Bravo-Suárez, J. J.; Páez-Mozo, E. A.; Oyama, S. T.; *Quim. Nova* **2004**, *27*, 601. [Crossref]

11. Basu, D.; Das, A.; Stöckelhuber, K. W.; Wagenknecht, U.; Heinrich, G.; *Prog. Polym. Sci.* **2014**, *39*, 594. [Crossref]
12. Bukhtiyarova, M. V.; Nuzhdin, A. L.; Bukhtiyarov, A. V.; Kardash, T. Y.; Romanenko, A. V.; *Catal. Commun.* **2019**, *127*, 39. [Crossref]
13. Nakagaki, S.; Castro, K. A. D. F.; Ucoski, G. M.; Halma, M.; Prévot, V.; Forano, C.; Wypych, F.; *J. Braz. Chem. Soc.* **2014**, *25*, 2329. [Crossref]
14. Berber, M. R.; Hafez, I. H.; *Bull. Environ. Contam. Toxicol.* **2018**, *101*, 751. [Crossref]
15. Qiao, W.; Bai, H.; Tang, T.; Miao, J.; Yang, Q.; *Colloids Surf., A* **2019**, *577*, 118. [Crossref]
16. do Amaral, L. F. M.; de Freitas, R. A.; Wypych, F.; *Appl. Clay Sci.* **2020**, *193*, 105660. [Crossref]
17. do Amaral, L. F. M.; Wypych, F.; de Freitas, R. A.; *Appl. Clay Sci.* **2021**, *201*, 105918. [Crossref]
18. Sun, Z.; Park, J. S.; Kim, D.; Shin, C. H.; Zhang, W.; Wang, R.; Rao, P.; *Water, Air, Soil Pollut.* **2017**, *228*, 23. [Crossref]
19. Huang, D.; Ma, J.; Fan, C.; Wang, K.; Zhao, W.; Peng, M.; Komarneni, S.; *Appl. Clay Sci.* **2018**, *152*, 230. [Crossref]
20. Zhou, H.; Jiang, Z.; Wei, S.; *Appl. Clay Sci.* **2018**, *153*, 29. [Crossref]
21. Zhou, H.; Jiang, Z.; Wei, S.; Liang, J.; *Water, Air, Soil Pollut.* **2018**, *229*, 78. [Crossref]
22. Xie, Y.; Yuan, X.; Wu, Z.; Zeng, G.; Jiang, L.; Peng, X.; Li, H.; *J. Colloid Interface Sci.* **2019**, *536*, 440. [Crossref]
23. Dias, A.; Cunha, L.; Vieira, A. C.; *Mater. Res. Bull.* **2011**, *46*, 1346. [Crossref]
24. Miyata, S.; *Clays Clay Miner.* **1983**, *31*, 305. [Crossref]
25. Badreddine, M.; Khaldi, M.; Legrouri, A.; Barroug, A.; Chaouch, M.; De Roy, A.; Besse, J. P.; *Mater. Chem. Phys.* **1998**, *52*, 235. [Crossref]
26. Szabados, M.; Mészáros, R.; Erdei, S.; Kónya, Z.; Kukovecz, Á.; Sipos, P.; Pálinkó, I.; *Ultrason. Sonochem.* **2016**, *31*, 409. [Crossref]
27. Radha, S.; Kamath, P. V.; *Cryst. Growth Des.* **2009**, *9*, 3197. [Crossref]
28. Prevot, V.; Forano, C.; Besse, J. P.; *Chem. Mater.* **2005**, *17*, 6695. [Crossref]
29. Prevot, V.; Briois, V.; Cellier, J.; Forano, C.; Leroux, F.; *J. Phys. Chem. Solids* **2008**, *69*, 1091. [Crossref]
30. Bhojaraj, J. A.; Kolinjavadi, M. R.; Rajamathi, M.; *ACS Omega* **2019**, *22*, 20072. [Crossref]
31. Kotas, J.; Stasicka, Z.; *Environ. Pollut.* **2000**, *107*, 263. [Crossref]
32. Frost, R. L.; Kloprogge, J. T.; *Spectrochim. Acta, Part A* **1999**, *55*, 2195. [Crossref]
33. Kloprogge, J. T.; Hickey, L.; Frost, R. L.; *Mater. Chem. Phys.* **2005**, *89*, 99. [Crossref]
34. Delgado, R. R.; Arandigoyen Vidaurre, M.; De Pauli, C. P.; Ulibarri, M. A.; Avena, M. J.; *J. Colloid Interface Sci.* **2004**, *280*, 431. [Crossref]
35. Kuang, J.; Ba, Z.; Li, Z.; Jia, Y.; Wang, Z.; *Surf. Coatings Technol.* **2019**, *361*, 75. [Crossref]
36. Liu, J.; Song, J.; Xiao, H.; Zhang, L.; Qin, Y.; Liu, D.; Hou, W.; Du, N.; *Powder Technol.* **2014**, *253*, 41. [Crossref]
37. Mathey, Y.; Greig, D. R.; Shriver, D. F.; *Inorg. Chem.* **1982**, *21*, 3409. [Crossref]
38. Poul, L.; Jouini, N.; Fievet, F.; *Chem. Mater.* **2000**, *12*, 3123. [Crossref]
39. Wang, N.; Cai, C.; He, X.; Pang, S.-F.; Zhang, Y.-H.; *Spectrochim. Acta, Part A* **2018**, *192*, 420. [Crossref]
40. Tackett, J. E.; *Appl. Spectrosc.* **1989**, *43*, 483.[Crossref]
41. Fahami, A.; Al-Hazmi, F. S.; Al-Ghamdi, A. A.; Mahmoud, W. E.; Beall, G. W.; *J. Alloys Compd.* **2016**, *683*, 100. [Crossref]
42. Manohara, G. V.; Vishnu Kamath, P.; Milius, W.; *J. Solid State Chem.* **2012**, *196*, 356. [Crossref]
43. Frost, R. L.; López, A.; Scholz, R.; Wang, L.; *Spectrochim. Acta, Part A* **2015**, *148*, 232. [Crossref]
44. Pang, S.-F.; Wu, C.-Q.; Zhang, Q.-N.; Zhang, Y.-H.; *J. Mol. Struct.* **2015**, *1087*, 46. [Crossref]
45. Ishioka, T.; Shibata, Y.; Takahashi, M.; Kanesaka, I.; Kitagawa, Y.; Nakamura, K. T.; *Spectrochim. Acta, Part A* **1998**, *54*, 1827. [Crossref]
46. Pokhriyal, M.; Uma, S.; Nagarajan, R.; *J. Rare Earths* **2017**, *35*, 474. [Crossref]
47. Heyrovska, R.; *Chem. Phys. Lett.* **2007**, *436*, 287. [Crossref]
48. Di Bitetto, A.; Kervern, G.; André, E.; Durand, P.; Carteret, C.; *J. Phys. Chem. C* **2017**, *121*, 6104. [Crossref]
49. Prasanna, S. V.; Kamath, P. V.; *Ind. Eng. Chem. Res.* **2009**, *48*, 6315. [Crossref]
50. Prasanna, S. V.; Kamath, P. V.; Shivakumara, C.; *J. Colloid Interface Sci.* **2010**, *344*, 508. [Crossref]
51. Costantino, U.; Vivani, R.; Bastianini, M.; Costantino, F.; Nocchetti, M.; *Dalton Trans.* **2014**, *43*, 11587. [Crossref]
52. Lv, L.; Wang, Y.; Wei, M.; Cheng, J.; *J. Hazard. Mater.* **2008**, *152*, 1130. [Crossref]
53. Szabados, M.; Varga, G.; Kónya, Z.; Kukovecz, Á.; Carlson, S.; Sipos, P.; Pálinkó, I.; *Ultrason. Sonochem.* **2018**, *40*, 853. [Crossref]
54. Koilraj, P.; Kannan, S.; *Chem. Eng. J.* **2013**, *234*, 406. [Crossref]
55. Bini, M.; Ambrogi, V.; Donnadio, A.; Di Michele, A.; Ricci, P.; Nocchetti, M.; *Appl. Clay Sci.* **2020**, *197*, 105796. [Crossref]
56. Yin, Q.; Zhang, J.; Luo, J.; Han, J.; Shao, M.; Wei, M.; *Chem. Eng. J.* **2020**, *389*, 124376. [Crossref]
57. Radha, S.; Antonyraj, C. A.; Kamath, P. V.; Kannan, S.; *Zeitschrift für Anorg. Chemie* **2010**, *636*, 2658. [Crossref]
58. Radha, S.; Kamath, P. V.; *Inorg. Chem.* **2013**, *52*, 4834. [Crossref]
59. Khaldi, M.; De Roy, A.; Chaouch, M.; Besse, J. P.; *J. Solid State Chem.* **1997**, *130*, 66. [Crossref]
60. Al-Jaberi, M.; Naille, S.; Dossot, M.; Ruby, C.; *J. Mol. Struct.* **2015**, *1102*, 253. [Crossref]

61. Bastianini, M.; Costenaro, D.; Bisio, C.; Marchese, L.; Costantino, U.; Vivani, R.; Nocchetti, M.; *Inorg. Chem.* **2012**, *51*, 2560. [Crossref]
62. Kang, J.; Levitskaia, T. G.; Park, S.; Kim, J.; Varga, T.; Um, W.; *Chem. Eng. J.* **2020**, *380*, 122408. [Crossref]
63. Dessalegne, M.; Zewge, F.; Pfenninger, N.; Johnson, C. A.; Diaz, I.; *Water, Air, Soil Pollut.* **2016**, *227*, 381. [Crossref]
64. Tammaro, L.; Vittoria, V.; Calarco, A.; Petillo, O.; Riccitiello, F.; Peluso, G.; *J. Dent.* **2014**, *42*, 60. [Crossref]
65. Mostarih, R.; de Roy, A.; *J. Phys. Chem. Solids* **2006**, *67*, 1058. [Crossref]
66. Zhang, H.; Wen, X.; Wang, Y.; *J. Solid State Chem.* **2007**, *180*, 1636. [Crossref]
67. Roonasi, P.; Holmgren, A.; *J. Colloid Interface Sci.* **2009**, *333*, 27. [Crossref]
68. Madhurambal, G.; Mariappan, M.; Hariharan, S.; Ramasamy, P.; Mojumdar, S. C.; *J. Therm. Anal. Calorim.* **2013**, *112*, 1031. [Crossref]
69. Legrouri, A.; Badreddine, M.; Barroug, A.; De Roy, A.; Besse, J. P.; *J. Mater. Sci. Lett.* **1999**, *18*, 1077. [Crossref]
70. de Oliveira, H. B.; Wypych, F.; *J. Solid State Chem.* **2016**, *243*, 136. [Crossref]
71. Cooper, M. A.; Hawthorne, F. C.; *Can. Mineral.* **1996**, *34*, 91. [Link] accessed in November 2022
72. Khaldi, M.; De Roy, A.; Chaouch, M.; Besse, J. P.; *Ann. Chim. Sci. Matériaux* **1998**, *23*, 337. [Crossref]
73. Iftekhar, S.; Küçük, M. E.; Srivastava, V.; Repo, E.; Sillanpää, M.; *Chemosphere* **2018**, *209*, 470. [Crossref]
74. Ookubo, A.; Ooi, K.; Tani, F.; Hayashi, H.; *Langmuir* **1994**, *10*, 407. [Crossref]
75. Yang, K.; Yan, L.; Yang, Y.; Yu, S.; Shan, R.; Yu, H.; Zhu, B.; Du, B.; *Sep. Purif. Technol.* **2014**, *124*, 36. [Crossref]
76. Zhang, Q.; Ji, F.; Zhao, T.; Shen, Q.; Fang, D.; Kuang, L.; Jiang, L.; Ding, S.; *Appl. Clay Sci.* **2019**, *174*, 159. [Crossref]
77. Sotiles, A. R.; Wypych, F.; *Chem. Commun.* **2019**, *55*, 7824. [Crossref]
78. Tsujimura, A.; Uchida, M.; Okuwaki, A.; *J. Hazard. Mater.* **2007**, *143*, 582. [Crossref]

Submitted: July 14, 2022
Published online: November 7, 2022

This is an open-access article distributed under the terms of the Creative Commons Attribution License.